

polymer papers

Poly-D(-)(3-hydroxybutyrate)/poly(ethylene oxide) blends: phase diagram, thermal and crystallization behaviour

Maurizio Avella and Ezio Martuscelli*

Istituto di Ricerche su Tecnologia dei Polimeri e Reologia del CNR, Via Toiano 6,
80072 Arco Felice, Napoli, Italy

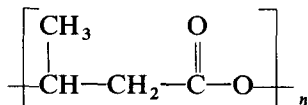
(Received 23 July 1987; revised 26 February 1988; accepted 13 April 1988)

Differential scanning calorimetry and optical microscopy were used to determine the miscibility behaviour of poly-D(-)(3-hydroxybutyrate) (PHB) and poly(ethylene oxide) (PEO) mixtures. It was found that PHB and PEO are miscible in the melt. Consequently the blend exhibits a single glass transition temperature and a depression of the equilibrium melting temperature of PHB. The study of the isothermal crystallization process shows that at a given crystallization temperature the presence of PEO causes a depression in the growth rate of PHB spherulites. The blend exhibits a phase diagram characterized by the presence, below the apparent melting temperature of PHB and PEO, of interlamellar and/or interfibrillar homogeneous amorphous PHB/PEO mixtures. The Flory-Huggins interaction parameter (χ_{12}), obtained from melting point depression data, is composition dependent, and its value is always negative.

(Keywords: poly-D-(3-hydroxybutyrate); poly(ethylene oxide); glass transition temperature; phase diagram; crystallization)

INTRODUCTION

Optically active poly-D(-)(3-hydroxybutyrate) (PHB) is a polyester produced via biosynthesis by bacterial fermentation¹. The molecular structure of PHB is:



It has been found that PHB is thermoplastic with a high degree of crystallinity and a well-defined melting point (around 180°C)². At relatively low undercooling, PHB crystallizes from the melt giving rise to the formation of large spherulites. The nucleation behaviour, the crystallization and the morphology of PHB have been studied by Barham *et al.*³.

Unlike other thermoplastic polymers, such as polypropylene and polyethylene, PHB is truly biodegradable and highly biocompatible.

Films of PHB show gas barrier properties comparable to poly(vinyl chloride) and poly(ethylene terephthalate). The combination of all these properties indicates that PHB may compete with commodity polymers in the packaging industry especially in areas where non-biodegradable plastic items, due to environmental pollution, are not allowed.

PHB can be injection moulded and extruded providing care is taken to minimize melt temperatures and residence time. It is melt unstable and degrades to crotonic acid if kept for a relatively long time at temperatures of only a few degrees above its melting point.

Injection-moulded PHB bars show a high crystallinity with a brittle behaviour, especially at temperatures below the glass transition temperature⁴.

Thus it may be concluded that PHB suffers two limitations in its use: a very narrow processability window, and a relatively low impact resistance.

From the above considerations, we have undertaken research with the aim of finding polymers suitable to be mixed with PHB to obtain new PHB-based materials with improved processability and impact resistance. The present paper reports on the results of an investigation concerning the thermal and crystallization behaviour of binary blends obtained by mixing PHB and poly(ethylene oxide) (PEO). The compatibility in the melt of PHB and PEO, together with the phase structure above and below the melting temperatures of the two polymers as function of composition, and the crystallization conditions and thermal history are also studied.

EXPERIMENTAL

Materials

The PHB sample used in the present papers was supplied by ICI. It was synthesized by the continuous fermentation of a glucose utilizing mutant of *Alcaligenes eutrophus*⁵. The molecular characteristics of PHB and PEO are shown in Table 1.

Table 1 Molecular characteristics, source and code of PHB and PEO

Polymer	Source	Code	Molecular mass
Poly-D(-)(3-hydroxybutyrate)	ICI (UK)	PHB	279 000 ^a
Poly(ethylene oxide)	Fluka-AG	PEO	20 000 ^b

^a By g.p.c. in chloroform at 30°C³

^b By intrinsic viscosity at 30°C in water⁶

* To whom correspondence should be addressed.

Table 2 Composition of PHB/PEO blends investigated, code and range of crystallization temperature (T_c) explored

Blend composition PHB/PEO (wt ratio)	Code	Range of T_c explored (°C)
100/0	PHB	90–140
80/20	PHB 80	100–130
60/40	PHB 60	100–125
40/60	PHB 40	95–120
20/80	PHB 20	90–120

Preparation of blends

Blends were prepared by slowly casting films from chloroform. The resulting films were dried under vacuum at 80°C until they reached constant weight. The composition of the blends investigated and the range of the crystallization temperature (T_c) explored are given in Table 2.

Measurements of radial growth rate of PHB spherulites

The radial growth rate of PHB spherulites was obtained by photographing, at a given T_c , the spherulites as function of time using an optical microscope. The radial growth rate ($G = dR/dt$) was calculated as the slope of the lines obtained by plotting the radius, R , against the time, t .

A Reichart polarizing optical microscope equipped with a Mettler hot stage (precision $\pm 0.2^\circ\text{C}$) was used.

The following procedure was followed. Thin films of PHB and PHB/PEO blends, as obtained by casting, were first heated to 200°C and kept at this temperature for 1 min. The temperature was rapidly lowered to the desired T_c and the PHB allowed to crystallize isothermally.

It is interesting to note that the T_c investigated for the determination of G was higher than the melting temperature of plain PEO.

As soon as the spherulites of PHB filled all the space available, that is impingement occurred, the temperature was raised and the melting point of the sample crystallized at T_c was optically measured by detecting the disappearance of the birefringence pattern.

During the thermal treatment the blend films were kept under a continuous stream of nitrogen in order to avoid degradation of polymers.

Differential scanning calorimetry and glass transition temperature measurements

Differential scanning calorimetry (d.s.c.) was used to study the influence of blend composition and thermal history on properties such as crystallinity and T_m and T_c of PHB and PEO. First the films obtained by casting were heated from 25 to 200°C (I run). The T_m of the PHB and PEO phase together with the corresponding crystallinity were determined from the d.s.c. endotherms. After 1 min at 200°C the samples were cooled down to room temperature (crystallization run) and the crystallization exotherms were registered. From this it was possible to derive the T_c of PHB and PEO. Finally the samples were heated to 200°C (II run). The melting point and the crystallinity of polymers after this thermal history were again measured. A scan rate of 20°C min⁻¹ was used throughout.

The glass transition temperature (T_g) of plain polymers

and blends was obtained by heating a sample first melted at 200°C and then rapidly quenched at -100°C.

A Mettler TA-3000 apparatus, equipped with a control and programming unit (microprocessor TC-10) and a calorimetric cell (DSC-30) that allows temperature scans from -170 to 600°C was used.

RESULTS AND DISCUSSION

Non-isothermal crystallization. Calorimetric studies

The d.s.c. thermograms of PHB and PHB/PEO films as obtained by casting show two distinct endotherm peaks when heated from room temperature to 200°C. The higher temperature peak represents the fusion of the PHB phase while that at lower temperature (around 60°C) the melting of the PEO phase. The apparent melting temperature (T'_m) of the PHB and PEO phase (I run), as shown by Figure 1, decreases with the increase of the second component content. As far as the T_g is concerned, it emerges from d.s.c. analysis that PHB/PEO blends are characterized by a single T_g intermediate between that of PHB and PEO. Moreover, as shown by Table 3, T_g is composition dependent.

Several theoretical and empirical equations have been used to describe the T_g - composition dependence of polymer/polymer blends. One of these, the Fox equation⁷, is written as:

$$1/T_g(\text{blend}) = W(\text{PHB})/T_g(\text{PHB}) + W(\text{PEO})/T_g(\text{PEO}) \quad (1)$$

where $T_g(\text{blend})$ is the glass transition temperature of the blend, $T_g(\text{PHB})$ and $T_g(\text{PEO})$ are those of plain PHB and

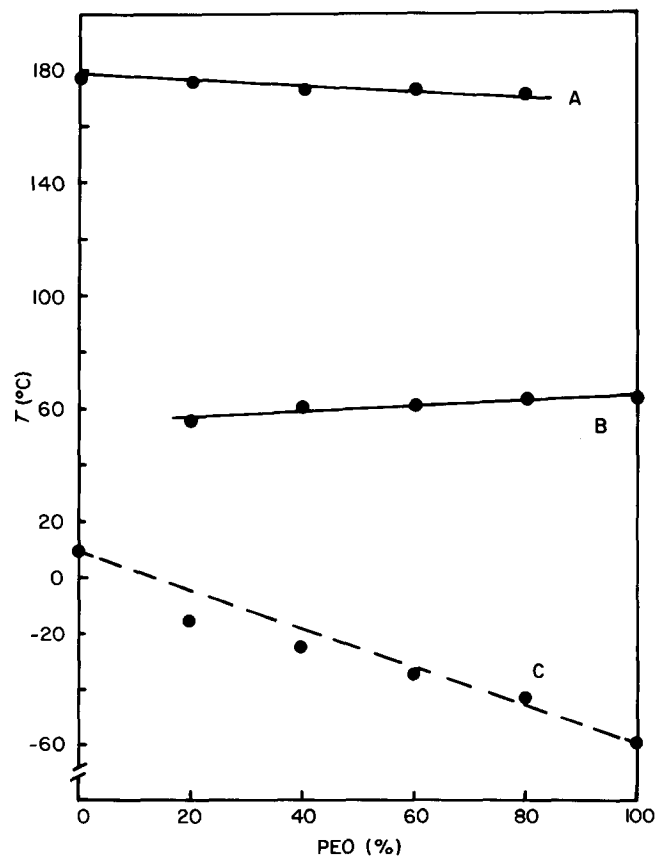
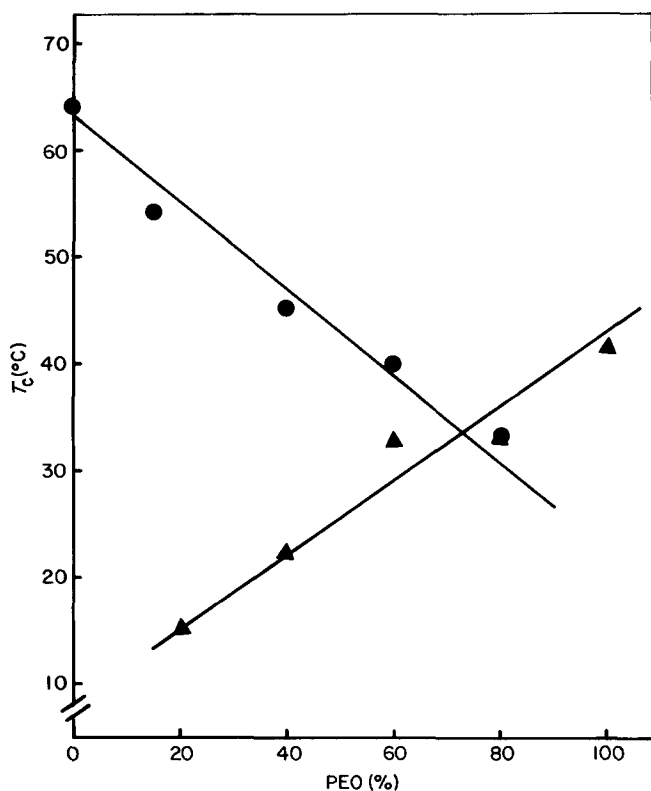


Figure 1 PHB/PEO phase diagram. A, T'_m PHB; B, T'_m PEO; C, T_g (expt), ---, T_g (Fox)

Table 3 Glass transition temperature (T_g) of plain PHB and PEO and of PHB/PEO blends

Sample	T_g (°C)
PHB	9
PHB 80	-15
PHB 60	-25
PHB 40	-34
PHB 20	-43
PEO	-59


Figure 2 Non-isothermal d.s.c. crystallization temperature (T_c) of PHB (●) and PEO (▲) as a function of blend composition

PEO, and $W(\text{PHB})$ and $W(\text{PEO})$ are the corresponding weight fractions.

Equation (1), as shown by *Figure 1*, fits the experimental T_g data quite well. The results strongly suggest that PHB and PEO are compatible in the melt and in the amorphous state. Thus it can be concluded that, between the T'_m lines of PHB and PEO, crystals of PHB coexist with a homogeneous PHB/PEO amorphous phase.

Below the PEO T'_m line, crystals of PHB and PEO together with a PHB/PEO amorphous phase are present. Finally, below the T_g line PHB and PEO crystalline phases coexist with a glassy homogeneous PHB/PEO phase.

The d.s.c. traces obtained during the non-isothermal crystallization run show the presence of two exothermic peaks corresponding to the crystallization of PHB and PEO. As shown by *Figure 2*, the temperature position of such a peak (T_c) is composition dependent. In both cases it can be observed that the T_c of the two polymers is sharply depressed by the presence of the second component (it may be noted that the PHB 20 blend shows only one crystallization peak).

Similar results were found by Martuscelli *et al.*⁸ in the case of PEO/PMMA blends. Such behaviour is related, as will be discussed next, to the depression of the spherulite growth rate due to the mutual dilution effect of the two polymers. The influence of melt compatibility on the primary nucleation processes should be also taken into account⁹. The d.s.c. mass crystallinity, as determined by first run traces on cast films, as a function of blend composition is shown in *Figure 3*.

The crystallinity of the PEO phase decreases with the increase of PHB in the blend. Such a result is probably accounted for by assuming that a fraction of PEO is not allowed to crystallize being trapped in the interlamellar amorphous regions of PHB spherulites giving rise, with uncrystallized PHB, to the formation of an homogeneous mixture. From the trend of the curves in *Figure 3* it is possible to conclude that while the fraction of PEO involved in the formation of the amorphous interlamellar mixture increases drastically with the content of the second component, that of PHB ranges from 50 to 61% with a maximum for the PHB 60 blend.

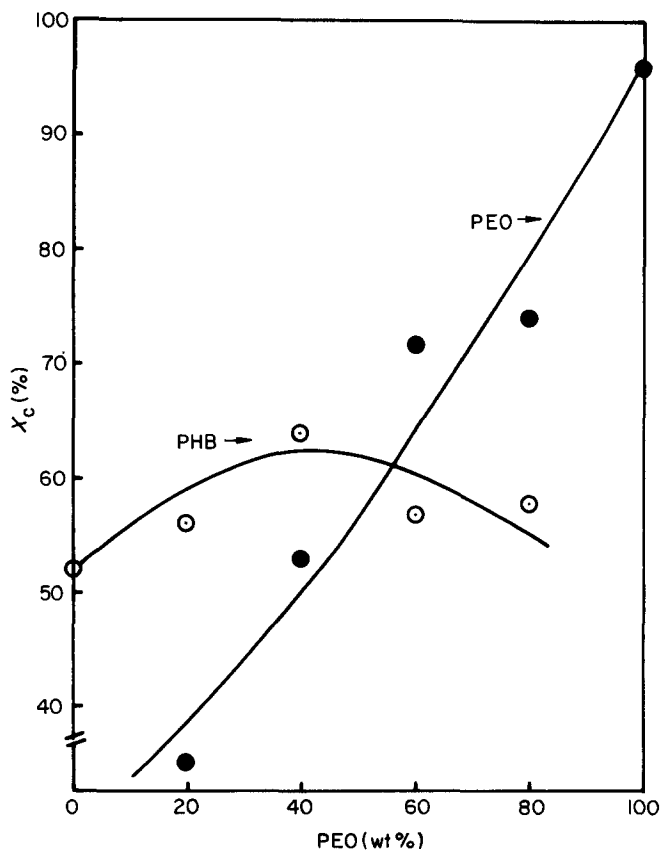
Isothermal crystallization

Equilibrium melting temperature and melting point depression. The T_m of PHB and PHB crystallized isothermally from its mixtures with PEO, as measured by optical microscopy, are plotted *versus* T_c in *Figure 4*.

The linear trend observed for all compositions shows that the Hoffman-Weeks¹⁰ equation:

$$T'_m = T_c/\gamma + (1 - 1/\gamma)T_m \quad (2)$$

fits the experimental data. Extrapolation to the line where $T'_m = T_c$ enables the equilibrium melting point to be


Figure 3 Phase crystallinity of PEO and PHB as function of blend composition

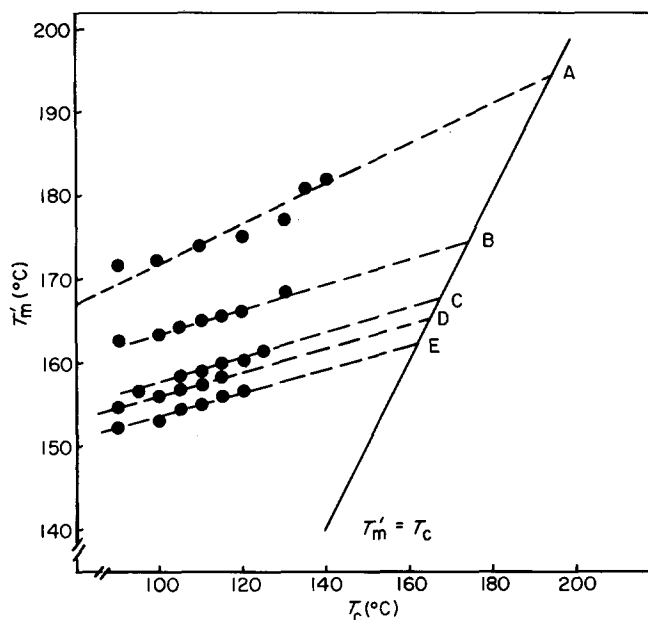


Figure 4 Plots of T_m' versus T_c used to determine the equilibrium melting point (T_m) of PHB for different blend compositions. A, PHB 100; B, PHB 80; C, PHB 60; D, PHB 40; E, PHB 20

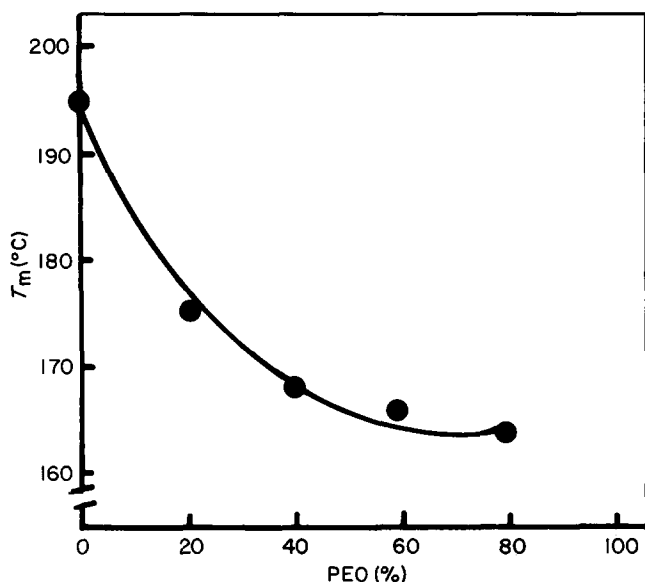


Figure 5 Plot of the equilibrium melting point (T_m) of PHB versus PEO content

obtained. The values of T_m determined by this method are reported for each blend in Table 4, and plotted versus the PEO content in Figure 5.

The equilibrium melting point found for the PHB investigated in this work (194°C) agrees quite well with the value ($195 \pm 5^\circ\text{C}$) obtained by Barham *et al.*³

From the data of Table 4 and the trend of Figure 5 it emerges that the addition of PEO causes a drastic depression in the T_m of PHB (T_m of plain PHB = 194°C ; T_m of PHB 20 = 163°C). Such a result indicates that PEO is able to act as a diluent for PHB and that the two polymers are compatible in the melt phase.

The melting point depression of a crystallizable polymer blended with an amorphous polymer in a compatible mixture, according to the Flory-Huggins theory^{11,12} can be written as:

$$\frac{1}{T_m} - \frac{1}{T_m^0} = -\frac{RV_2}{\Delta H^0 V_1} \left[\frac{\ln \Phi_2}{m_2} + \left(\frac{1}{m_2} - \frac{1}{m_1} \right) \Phi_1 + \chi_{12} \Phi_1^2 \right] \quad (3)$$

where T_m and T_m^0 are the equilibrium melting points of the blend and homopolymer, respectively, ΔH^0 is the heat of fusion for the 100% PHB, V_1, V_2 are the molar volumes of the repeat units of PEO and PHB, respectively, m_1, Φ_1 and m_2, Φ_2 are the degree of polymerization and the volume fractions of the non-crystallizable (PEO) and crystallizable polymers (PHB). Equation (3) may be applied to PHB/PEO blends because the T_c investigated was above the T_m^0 of PEO. Thus, under such conditions PEO is non-crystallizable. By rearranging the terms, equation (3) can be written as:

$$-\left[\frac{\Delta H^0 V_1}{RV_2} \left(\frac{1}{T_m} - \frac{1}{T_m^0} \right) + \frac{\ln \Phi_2}{m_2} + \left(\frac{1}{m_2} - \frac{1}{m_1} \right) \Phi_1 \right] = \chi_{12} \Phi_1^2 \quad (4)$$

Equation (4) can be used to estimate the PEO-PHB interaction parameter χ_{12} . If χ_{12} is composition independent and the melting point depression is not influenced by morphological effects then a plot of the left-hand side of equation (4) versus Φ_1^2 , should give a straight line passing through the origin. The slope of such line gives χ_{12} .

In order to calculate the left-hand side term of equation (4), the following parameter values have been used: $\Delta H^0 = 3001 \text{ cal mol}^{-1}$; $V_1 = 44 \text{ cm}^3 \text{ mol}^{-1}$; $V_2 = 75 \text{ cm}^3 \text{ mol}^{-1}$; $m_1 = 454$ and $m_2 = 3245$.

For V_1 (molar volume of PEO) a value of $44 \text{ cm}^3 \text{ mol}^{-1}$ was used. This value, experimentally determined by a dilatometric technique, corresponds to the molar volume at 180°C , that is, around the T_m of PHB¹³. For V_2 (molar volume of PHB) a value of $75 \text{ cm}^3 \text{ mol}^{-1}$ was used. This value was calculated by using the amorphous density of PHB (1.15 g cm^{-3}) (ref. 3).

The plot of equation (4) obtained by using the values of T_m^0 (PHB) and T_m (blend) experimentally found (see Table 4) is shown in Figure 6. The experimental points may be interpolated by a line with an intercept at origin of 0.094 and a slope of -0.075 . The fact that this line does not pass through the origin can be accounted for by a composition dependence of χ_{12} . If this is the case then the interaction parameter, at different blend composition, can be obtained as the slope of the broken lines in Figure 6¹².

The values of χ_{12} calculated according to this method are reported as function of composition in Table 5. The finding that χ_{12} is negative for all investigated compositions strongly indicates that in the melt, at T_m , PHB and PEO are compatible.

Radial growth rate of PHB spherulites. As shown by the optical micrograph series in Figure 7, PHB is able to

Table 4 Equilibrium melting temperature (T_m) for plain PHB and for PHB/PEO blends

Sample	T_m ($^\circ\text{C}$)
PHB	194
PHB 80	175
PHB 60	168
PHB 40	166
PHB 20	163

crystallize according to a spherulitic morphology even in the case of the PHB 20 blend. It is interesting to note that no evidence of phase separation of PEO in the melt before and during crystallization of PHB is observed. This as already mentioned suggests that during crystallization PEO molecules are trapped between the PHB lamellae since the PHB spherulites fill the volume.

Attempts were made to grow PEO spherulites by lowering the temperature of the films, after complete crystallization of PHB, to room temperature, but this was unsuccessful. Such behaviour could be accounted for by

Table 5 Values of interaction parameter $\chi_{1,2}$, obtained from equation (4) and Figure 6, as a function of blend composition Φ_1

Blend	Φ_1	$\chi_{1,2}$
PHB 80	0.2	-2.00
PHB 60	0.4	-0.71
PHB 40	0.6	-0.34
PHB 20	0.8	-0.21

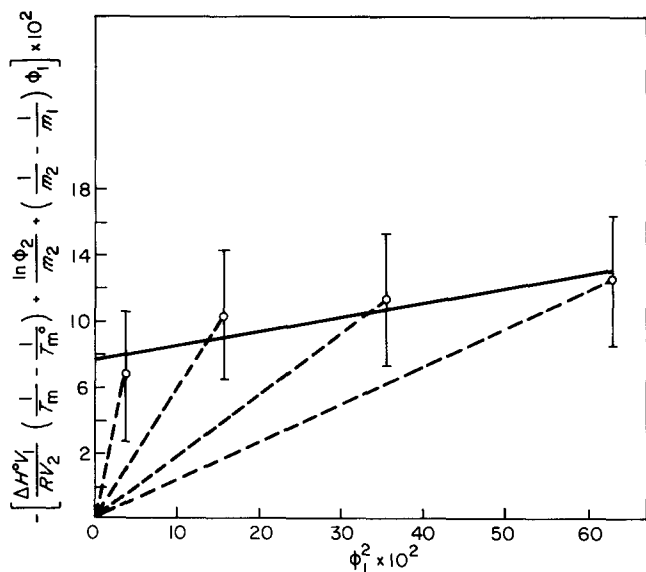


Figure 6 Plot of the left-hand side of equation (4) versus Φ_1^2

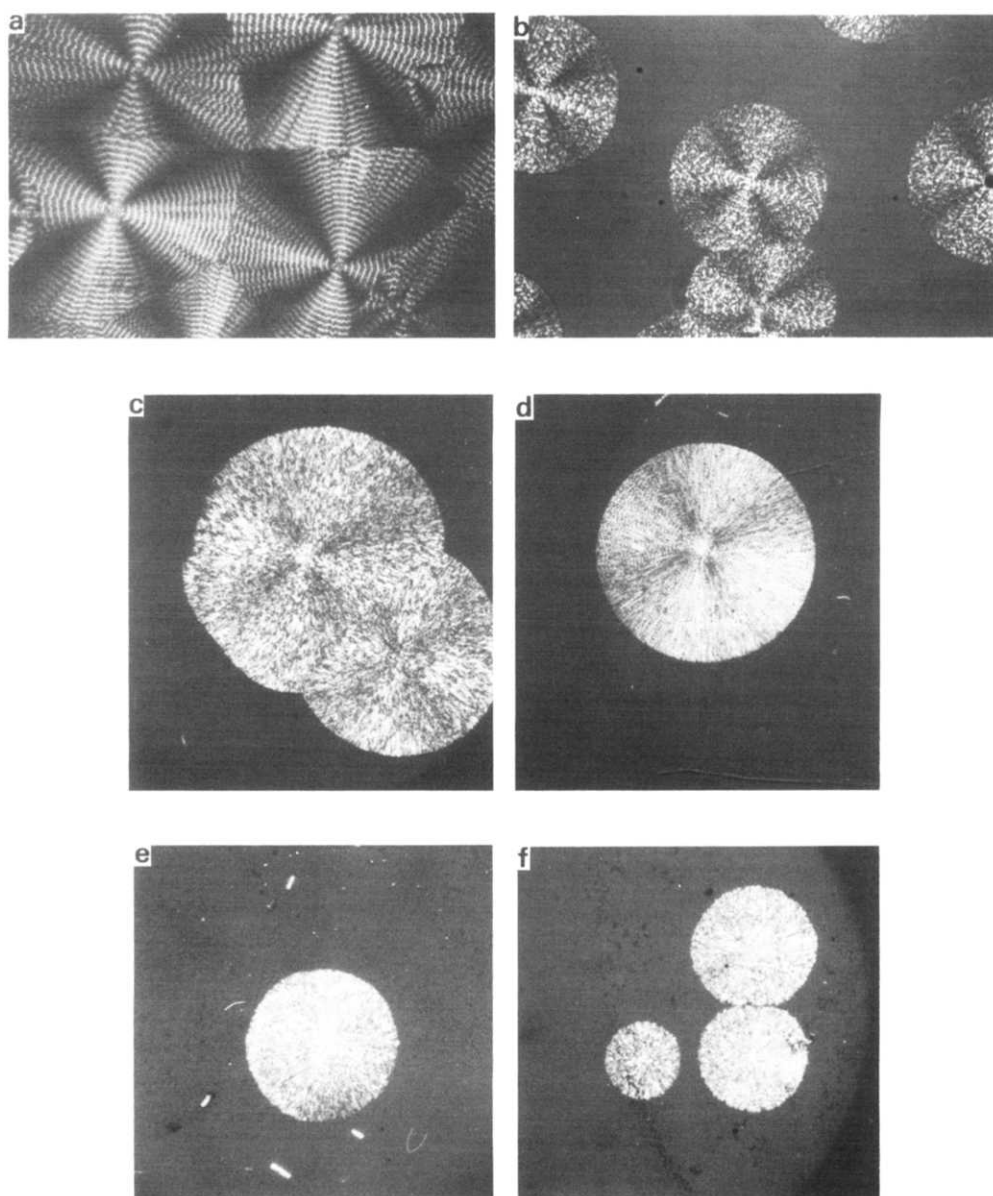


Figure 7 Optical micrographs of PHB spherulites grown isothermally at different temperatures and blend compositions. (a) PHB 100, $T_c=90^\circ\text{C}$; (b) PHB 100, $T_c=115^\circ\text{C}$; (c) PHB 80, $T_c=130^\circ\text{C}$; (d) PHB 60, $T_c=125^\circ\text{C}$; (e) PHB 40, $T_c=115^\circ\text{C}$; (f) PHB 20, $T_c=115^\circ\text{C}$

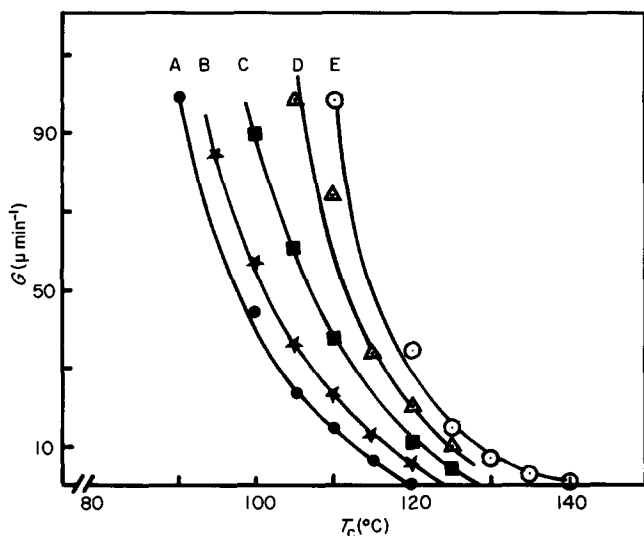


Figure 8 Radial growth rates (G) of PHB spherulites versus crystallization temperature (T_c) for the various blend compositions. A, PHB 20/PEO 80; B, PHB 40/PEO 60; C, PHB 60/PEO 40; D, PHB 60/PEO 40; E, PHB 100

assuming that PEO is unable to crystallize from PHB/PEO blends according to a spherulitic morphology. It is likely that only tiny crystals of PEO can grow in interlamellar regions of PHB spherulites. Work is in progress in order to verify this hypothesis.

Plots of the radius of the PHB spherulites against time for all blend compositions and T_c explored result in straight lines. This means that the concentration of PHB crystallizable molecules at the growth front is constant during the crystallization process. Thus, part of PEO molecules must diffuse away from the growth front to interlamellar or interfibrillar intraspherulitic regions. Plots of the spherulite radial growth rate, G , for various composition blends as a function of T_c are shown in Figure 8. From the trend of the curves in Figure 8 it emerges that the addition of PEO to PHB produces, at a given T_c , a depression in the G values. This effect, as shown by Figure 9, is composition dependent and for the range of T_c explored is more relevant at higher undercooling. It must be pointed out that G was measured in all cases at relatively low undercooling where the negative temperature dependence of G is controlled mainly by the secondary nucleation rate.

As already discussed in a previous paper¹⁴, the spherulite growth rate curves for a polymer/diluent system can be conveniently analysed by using the following growth rate expression¹⁵⁻¹⁷:

$$\lg G - \lg \Phi_2 + \frac{U^*}{2.3R(T_c - T_\infty)} - \frac{0.2T_m \ln \Phi_2}{2.3\Delta T} = \lg G_0 - \frac{k_g}{2.3T_c \Delta T f} \quad (5)$$

where G_0 is a pre-exponential factor, ΔT the undercooling and Φ_2 the volume fraction of PHB.

The $U^*/R(T_c - T_\infty)$ term contains the contribution of diffusional processes of the crystallizable (PHB) and non-crystallizable (PEO) components to the growth rate¹⁴. The quantity U^* represents the sum of the activation energies for the chain motion in the melt of PHB and PEO molecules. The temperature below which such segmental motion stops is indicated as T_∞ ($T_\infty =$

$T_g - C$)¹⁵. The quantity f is the correction factor for the heat of fusion, it takes into account the temperature dependence of ΔH^0 . Usually the following empirical expression is used for f :

$$f = 2T_c/T_m^0 + T_c$$

k_g is the nucleation factor containing the surface free energies σ and σ_e , equilibrium melting point T_m , heat of fusion ΔH^0 , thickness of the macromolecular layer b_0 and the Boltzmann constant K :

$$k_g = \frac{nb_0\sigma\sigma_e T_m}{\Delta H^0 K} \quad (6)$$

In equation (6), according to the Hoffman theory¹⁵, $n=4$ when the crystallization process conforms to regime I (low undercooling) and regime III (very high undercooling). For regime II (intermediate undercooling), n will assume a value of 2.

The procedure for determining k_g involves plotting the left-hand side term of equation (5) versus $1/T_c \Delta T f$ with the values of U^* and C chosen to give the best fit least squares line through the data. A very good fit is obtained when U^* ranges between 1000 cal mol⁻¹ and 1500 cal mol⁻¹ and $C = 51.6$ K (see Figure 10).

The values of k_g , calculated from the slopes of the lines of Figure 10, are reported in Table 6. It can be observed that the k_g value of plain PHB is about double that of blends.

Barham *et al.*³ found that PHB crystallizes according to regime III at the undercooling used in this study. This means that for PHB in equation (6), $n=4$. Taking into consideration this finding and the data of Table 6 it must be concluded that PHB crystallizes from its blends with PEO according to regime II ($n=2$ in equation (6)). Such results may probably be accounted for by the fact that the values of ΔT used in the case of PHB/PEO blends (60–

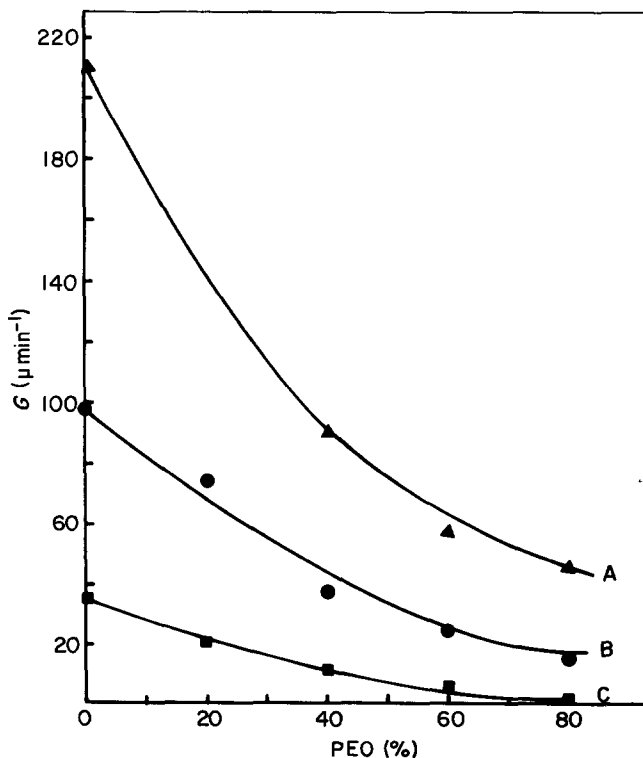


Figure 9 Plots of radial growth rates (G) of PHB spherulites against PEO content (wt %) at given T_c : A, 100; B, 110; C, 120°C

curve interpolates the G values of plain PHB. This result is most likely accounted for by the fact that in *Figure 11*, G values of blends, crystallizing according to regime II, are compared with those of plain PHB that crystallizes according to regime III.

CONCLUSIONS

From the results reported, it is possible to conclude that PHB and PEO are compatible in the melt state. Consequently the blend exhibits a single T_g , and depression of the T'_m and T_m values of PHB. Isothermal crystallization experiments have shown that at a given T_c , the presence of PEO causes a depression in the spherulite growth rate of PHB that increases with the content of PEO. Due to the change in T_m with composition, at the same T_c , blends crystallize according to regime II while PHB crystallizes according to regime III.

The PHB-PEO interaction parameter, obtained from melting point depression data results, is found to be composition dependent, and its value is always negative. This finding indicates that some kind of molecular interaction must be present. The specific interactions responsible for the PHB-PEO miscibility are likely to involve the carbonyl groups of the PHB and the hydrogen of the CH_2 group in PEO.

The thermal behaviour of the blends suggests a phase diagram characterized by the presence, below the T_m of PHB and PEO of interlamellar and/or interfibrillar homogeneous uncrystallized PHB/PEO mixtures. Work is in progress to confirm the hypothesis raised.

REFERENCES

- 1 Lemoigne, M. *Ann. Inst. Past.* 1925, **39**, 144; Merrick, J. *Photosynth. Bact.* 1978, **199**, 219; Dawes, E. A. and Senior, P. J. *Adv. Microbiol.* 1973, **10**, 138; Herron, J. S., King, J. D. and White, D. C. *Appl. Environ. Microbiol.* 1978, **35**, 251; Carr, N. G. *Biochem. Biophys. Acta* 1966, **120**, 308; Wallen, L. L. and Rohwedder, W. K. *Environ. Sci. Technol.* 1974, **8**, 576; Ward, A. C., Rowley, B. I. and Dawes, E. A. *J. Gen. Microbiol.* 1977, **102**, 61
- 2 Lundgren, D. G., Alper, R., Schnaitman, C. and Marchessault, R. H. *J. Bacteriol.* 1965, **89**, 245; Holmes, P. A., Wright, L. F. and Alderson, B. *Eur. Patent Application* 1979, 15123; Baptist, J. N. US Patent 1962, 3044942; *idem* US Patent 1962, 3036959; Lafferty, R. M. *Chem. Rundsch.* 1977, **30**, 15; Ellar, D., Lundgren, D. G., Okamura, K. and Marchessault, R. H. *J. Mol. Biol.* 1968, **35**, 489
- 3 Barham, P. J., Keller, A., Otun, E. L. and Holmes, P. A. *J. Mater. Sci.* 1984, **19**, 2781; Barham, P. J. *ibid.* 1984, **19**, 3826
- 4 Howells, E. R. *Chem. Ind.* 1982, 508
- 5 Hughes, L. and Richardson, K. R. *Eur. Patent Application* 1982, 46, 344
- 6 Bailey, F. E. and Koleske, J. V. 'Poly(ethylene oxide)', Academic Press, New York, 1976
- 7 Fox, T. G. *Bull. Am. Phys. Soc.* 1956, **2**, 123
- 8 Addonizio, M. L., Martuscelli, E. and Silvestre, C. *Polymer* 1987, **28**, 183
- 9 Bartczak, Z. and Martuscelli, E. *Makromol. Chem.* 1987, **188**, 445
- 10 Hoffman, J. D. and Weeks, J. J. *J. Res. Natl. Bur. Stand.* 1962, **66**, 13
- 11 Flory, P. J. 'Principles of Polymer Chemistry', Cornell University Press, Ithaca, 1953
- 12 Nishi, T. and Wang, T. T. *Macromolecules* 1975, **8**, 909
- 13 Cimmino, S., Martuscelli, E. and Silvestre, C. unpublished data
- 14 Cimmino, S., Martuscelli, E., Silvestre, C., Canetti, M., De Lalla, C. and Seves, A. *J. Polym. Sci., Polym. Phys. Edn.* submitted
- 15 Hoffman, J. D. *Polymer* 1983, **24**, 3
- 16 Boon, J. and Azcue, J. M. *J. Polym. Sci. (A2)* 1968, **6**, 885
- 17 Martuscelli, E. *Polym. Eng. Sci.* 1984, **24**, 563

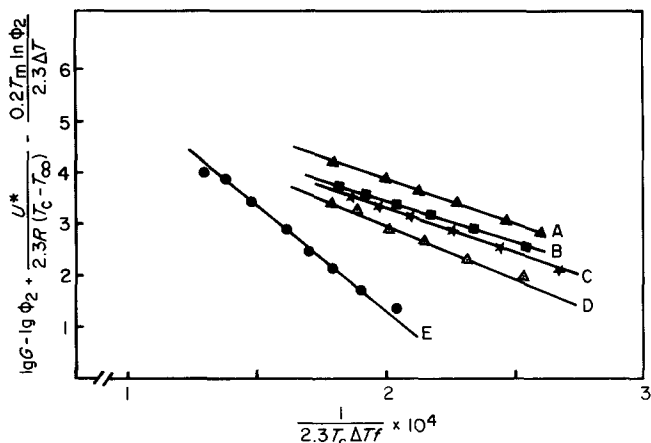


Figure 10 Plots of the left-hand side of equation (5) versus $1/fT_c\Delta T$ for plain PHB and PHB/PEO blends. A, PHB 20; B, PHB 40; C, PHB 60; D, PHB 80; E, PHB

Table 6 Values of the quantity k_g for plain PHB and for PHB/PEO blends

Blend	k_g (K^2)
PHB	3.8×10^5
PHB 80	2.0×10^5
PHB 60	1.8×10^5
PHB 40	1.6×10^5
PHB 20	2.0×10^5

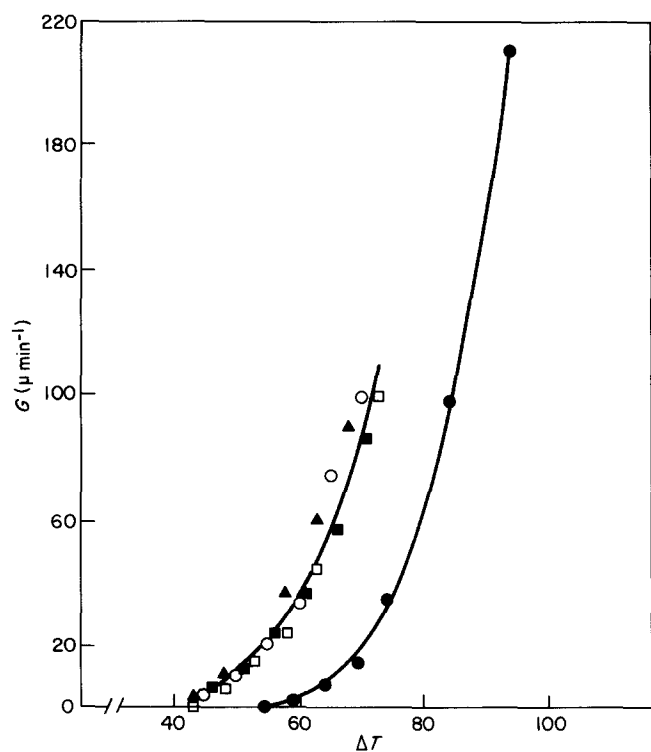


Figure 11 Plots of radial growth rates (G) for PHB and for PHB/PEO blends versus undercooling (ΔT). ●, PHB; ○, PHB 80; ▲, PHB 60; ■, PHB 40; □, PHB 20

30°C) are relatively lower than those used for plain PHB (105 – 55°C).

In *Figure 11* the growth rate of PHB spherulites is plotted as a function of undercooling ΔT . It can be observed that for all blends the data points are interpolated by the same curve. This finding indicates that, for the range of ΔT investigated, the main factor in determining the growth rate behaviour is the change in equilibrium melting point with composition. A distinct